



This is the accepted manuscript made available via CHORUS. The article has been published as:

# Unpaired Majorana Modes in Josephson-Junction Arrays with Gapless Bulk Excitations

M. Pino, A. M. Tsvelik, and L. B. Ioffe

Phys. Rev. Lett. **115**, 197001 — Published 6 November 2015

DOI: [10.1103/PhysRevLett.115.197001](https://doi.org/10.1103/PhysRevLett.115.197001)

# Unpaired Majorana modes in Josephson junctions arrays with gapless bulk excitations

M. Pino,<sup>1</sup> A. M. Tsvelik,<sup>2</sup> and L. B. Ioffe<sup>1,3</sup>

<sup>1</sup>*Department of Physics and Astronomy, Rutgers The State University of New Jersey,  
136 Frelinghuysen rd, Piscataway, 08854 New Jersey, USA*

<sup>2</sup>*Department of Condensed Matter Physics and Materials Science,  
Brookhaven National Laboratory, Upton, New York 11973-5000, USA*

<sup>3</sup>*CNRS, UMR 7589, LPTHE, F-75005, Paris, France.*

The search for Majorana bound states in solid-state physics has been limited to materials which display a gap in their bulk spectrum. We show that such unpaired states appear in certain quasi-one-dimensional Josephson junctions arrays with gapless bulk excitations. The bulk modes mediate a coupling between Majorana bound states via the Ruderman-Kittel-Yosida-Kasuya mechanism. As a consequence, the lowest energy doublet acquires a finite energy difference. For realistic set of parameters this energy splitting remains much smaller than the energy of the bulk eigenstates even for short chains of length  $L \sim 10$ .

PACS numbers: 74.81.Fa, 71.27.+a, 74.40.Kb, 85.25.Cp

*Introduction.* An intensive search for Majorana fermions [1] is underway in solid-state devices [2]. The vast majority of the proposals consist in zero energy boundary modes in materials with a gaped bulk spectrum. Spin-less superconducting wire and topological insulator in two or three dimensions fall in this category [3–5].

We propose an alternative approach for the observation of Majorana fermions in Josephson Junctions Arrays (JJA). We will show that certain quasi-one-dimensional JJA can display Majorana modes algebraically located at their boundaries. These Majorana fermions are emergent particles nonlocal with respect to quasi-particles, they emerge as a result of strong interactions taking place at the junctions of three JJ chains. They do not mix with higher energy excitations although bulk spectrum is not gapped. The existence of low-energy Majorana fermion could then be proved by spectroscopy [6, 7].

In this letter, we first explain the JJA system and how to model it with an Ising-like Hamiltonian. Then, a qualitative argument is employed to obtain the low-energy effective theory using unpaired Majorana modes. Numerical results will confirm the validity of this effective theory and show that Majorana modes are indeed protected. Finally, we discuss problems that may arise in the experimental realization of our proposal.

*Experimental set-up* We consider three identical ladders of Josephson junctions coupled together as in Fig. (1a) [8]. Each ladder has a unit cell with "large" and "small" junctions, Fig. (1b). Their corresponding Josephson energies are  $E_{JL}$  and  $E_{JS}$ , where  $E_{JL} > E_{JS}$ . The three ladders are closed at the ends by a junction with Josephson energy  $E_{JE}$ . We assume that charging energies are much smaller than Josephson ones for all the junctions. All the closed circuit in the ladders are at full frustration, that is, they are threaded by a magnetic flux equal to half of the flux quantum. The two larger loops are threaded by magnetic fluxes  $\varphi_1$  and  $\varphi_2$ , respectively.

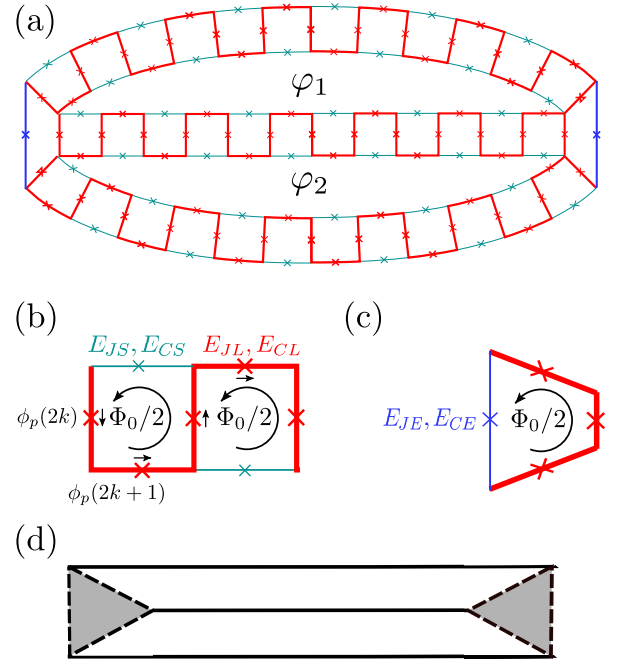


FIG. 1. (a) Three ladders of Josephson junctions coupled together. The two large loops are threaded by magnetic fluxes  $\varphi_1$  and  $\varphi_2$ . (b) Unit cell of one ladder. Josephson energy of "large" junction (red) is larger than the one of a "small" junction (green),  $E_{JL} > E_{JS}$ . All the cells are threaded by a magnetic flux equal to half of the flux quantum. (c) Loop at the boundaries. The Josephson coupling for the blue junction at the chains end is denoted as  $E_{JE}$ . (d) At low temperature and near a phase transition, the three Josephson ladders system maps to three Ising chains with transverse field (solid lines) and coupling between their ends (dotted lines). Majorana zero modes are algebraically located at the chains ends (dark regions).

For ladder  $p$ , the phase difference in the left vertical and horizontal red junctions in the loop  $k$  are denoted by

$\phi_p(2k)$  and  $\phi_p(2k+1)$ , respectively (see Fig. 1b).

At full frustration, the properties of one infinite chain are invariant under translation by one small closed loop and reflection through horizontal axes. We analyze the energy of one unit cell as a function of the phase difference in the "large" junctions:

$$\mathcal{U}_{p,k} = -E_{JL} \left\{ \cos[\phi_p(2k)] + \cos[\phi_p(2k+1)] \right\} + E_{JS} \cos[\phi_p(2k) + \phi_p(2k+1) + \phi_p(2k+2)], \quad (1)$$

where  $\mathcal{U}_{p,k}$  is the energy of the loop  $k$  of ladder  $p$ . The total energy has a global  $\mathbb{Z}_2$  symmetry given by  $\phi_p(i) = -\phi_p(i)$  in each junction  $i$ . In the regime  $E_{JL} \gg E_{JS}$ , the ground-state corresponds to all phases equal to zero  $\phi_p(i) = 0$  and the symmetry is preserved. However, a broken symmetry phase occurs for  $E_{JL} \ll E_{JS}$ , as in this regime the ground-state acquires a  $\phi_p(i) \neq 0$ . The critical point is located near  $E_{JL}/E_{JS} \sim 5$  [8]. The model (1) assumes low transparency junctions that are well described by  $\cos(\phi)$  energy, the presence of small higher harmonics does not change the results.

The specific details of the system are irrelevant near the phase transition and the properties of one ladder are described by an Ising chain with transverse field. The mapping can be written explicitly by taking each "large junction" as a 1/2-spin with component  $\sqrt{1 - \phi_p^2(i)}$  in the direction of the field. Near the phase transition, only the lowest non-zero order in the phase differences in "large" junctions are relevant. Then, the first term in Eq. (1) represents the field contribution and the second the Ising coupling between nearby spins (see supplemental material of Ref. [8] for details).

The junctions located at the ends of the chains, blue crosses in Fig. (1d), couple the three ladders:

$$\mathcal{U}_c = E_{JE} \left\{ \cos[\phi_1(1) + \phi_2(1) + \phi_3(1)] + \cos[\phi_1(L) + \phi_2(L) + \phi_3(L)] \right\}, \quad (2)$$

where  $L$  is the double of the number of squares in each ladder. This contribution gives an extra coupling between spins at the boundaries in the Ising model.

*Effective model.* Near the phase transition, the Hamiltonian of the three ladders of JJA maps to three Ising chains with transverse magnetic field and coupling between their ends  $H = \sum_p H_p + H_c$ , where:

$$H_p = -J \sum_{k=1}^{L-1} \sigma_p^x(k) \sigma_p^x(k+1) - h \sum_{k=1}^L \sigma_p^z(k), \quad (3)$$

$$H_c = -J_c \sum_{p=1}^3 \sigma_p^x(1) \sigma_{p+1}^x(1) + \sigma_p^x(L) \sigma_{p+1}^x(L). \quad (4)$$

We take index  $p$  module 3. The length of each chain is  $L$  and thus, the total number of sites of the three chains

is  $N = 3L$ . The Pauli matrices  $\sigma_a^z(i), \sigma_a^x(i), \sigma_a^y(i)$  act on spin at site  $i$  of chain  $p$ . The parameters  $J$  and  $h$  control the usual Ising interaction and magnetic field in the transverse axis, respectively. They can be related to the Josephson energies as  $J/h \sim E_{JL}/E_{JS}$ . The value of  $J_c$  sets the strength of the coupling between different chains and fulfills  $J_c/J \sim E_{JE}/E_{JL}$ . We are interested in the regime  $h/J \sim 1$  and  $J_c/J \sim 1$ . A schematic representation of the Hamiltonian appears in Fig. (1d).

There may be other small terms in our Hamiltonian for realistic experiments. We will comment later on different sources of incoherent behaviour and how they can affect the low-energy physics of Eqs. (1,2).

We express the low-energy degrees of freedom for Hamiltonian Eq. (3,4) in terms of Majorana fermions. We remark that Majorana fermions appearing in the low-energy effective theory of the JJA are nonlocal with respect to the Bogolyubov quasiparticles of the superconductors. This is an important difference between our case and the well-known case of 1D spinless superconductors. We use a multichannel version of the Jordan-Wigner transformation [9]. This mapping requires to enlarge the Hilbert space with an extra 1/2-spin. Operators acting on this spin are denoted by  $\sigma^x(0), \sigma^y(0)$  and  $\sigma^z(0)$ . The original spin operators are mapped to fermions via:

$$c_p^\dagger(k) = \eta_p(-1)^{\sum_{j<k} n_p(j)} \sigma_p^+(k), \quad (5)$$

where  $n_p(j) = [\sigma_j^z(p) + 1]/2$ . The  $\eta_p$  acts on the added 1/2 spin. They are:

$$\begin{aligned} \eta_1 &= \sigma^x(0) (-1)^{N_2+N_3}, \\ \eta_2 &= \sigma^y(0) (-1)^{N_1+N_3}, \\ \eta_3 &= \sigma^z(0) (-1)^{N_1+N_2}, \end{aligned}$$

where  $N_p$  is the total number of fermions in chain  $p$ . The operators defined in Eq (5) fulfill the fermionic algebra. Finally, Majorana fermions are defined as  $\psi_p(2k-1) = c_p(k) + c_p^\dagger(k)$  and  $\psi_p(2k) = i[c_p(k) - c_p^\dagger(k)]$ .

We focus on the regime in which each of the Ising chains are critical,  $J = h$ . Critical behavior for one single JJ chain has been experimentally proven in Ref. [8]. In this case, our model can be written as:

$$iH = J \sum_{j=1}^{2L} \vec{\psi}(j) \vec{\psi}(j+1) + \quad (6)$$

$$J_c \sum_{abc} \epsilon_{abc} \eta_b \eta_c [\psi_b(1) \psi_c(1) + \psi_b(2L) \psi_c(2L) (-1)^{N_b+N_c}],$$

where  $\vec{\psi}(j) = (\psi_1(j), \psi_2(j), \psi_3(j))$ . The coupling at the left boundary is  $\vec{S} \cdot (\vec{\psi}(1) \times \vec{\psi}(1))$ , where  $S^a = (i/2) \epsilon_{abc} \eta_b \eta_c$ . If only this coupling is considered, the Hamiltonian describes an over-screened two-channel Kondo (2CK) model [10–13]. The role of the impurity is played by the 1/2-spin  $\vec{S}$  and the relevant degrees of

freedom of the conduction electrons are described by the bulk spins of the three Ising chains. At temperatures below the Kondo temperature  $T_K \sim J \exp(-\text{const} J/J_c)$  the two-channel Kondo model displays the universal quantum critical behavior. At the Quantum Critical point (QCP), the 2CK model possesses a finite ground state entropy  $\ln \sqrt{2}$  which originates from the presence of a zero energy Majorana mode. This mode presents what is left from the impurity spin  $S=1/2$ . The leading irrelevant operator at the QCP describes a coupling of this mode to the product of three bulk Majorana at the impurity point.

It stands to reason that at  $L \rightarrow \infty$  model (6) describes two independent 2CK models. Formally such decoupling is achieved by declaring  $(-1)^{N_a} \eta_a$  as an independent Majorana fermion. Then its anti-commutator with  $\eta_a$  is zero on average. At finite  $L$ , Hamiltonian (6) possesses an additional energy scale generated by a tunneling between the Majorana modes located at different ends of the system. Below this scale one has to see deviations from the 2CK physics. These arguments assume that  $L > J/T_K$ , so that there is separation between energy scales associated with the Kondo physics and the ones associated with the Majorana fermions, the condition that is easy to achieve in practice.

Although model (6) is not integrable, we can analyze qualitatively the low-energy theory starting from the strong coupling limit  $J/J_c = 0$ . There are Majorana fermions at each end of the chains, (9)  $\mu_L = i\psi_1(1)\psi_2(1)\psi_3(1)$  and  $\mu_R = i\psi_1(2L)\psi_2(2L)\psi_3(2L)$ , which commute with the strong coupling Hamiltonian. That implies a two-fold degeneracy of the whole spectrum. Indeed, the occupancy of the fermionic state  $f = [\mu_L - i\mu_R]$  does not affect the energy. We notice that the fermion  $f$  is constructed from Majorana at different ends of the chain.

If one adopts the hypothesis of independence of two 2CK QCPs at  $L \rightarrow \infty$  and consider the finite size effects as a perturbation their contribution to the low-energy dynamics can be extracted from the effective Hamiltonian computed as [11]:

$$H_r \sim T_K^{-1/2} [\mu_L \psi_1(2)\psi_2(2)\psi_3(2) + \mu_R \psi_1(2L-1)\psi_2(2L-1)\psi_3(2L-1)]. \quad (7)$$

We expect that Majorana at each end couple via RKKY mechanism through the low-energy excitations [14–17]. Indeed, integrating over the fermions in (7) we obtain the effective Hamiltonian for the Majorana modes:  $H_{eff} = it\mu_L\mu_R$  where  $T \sim T_K^{-1} \int G(L, t)^3 dt \sim T_K^{-1} (v_F/L)^2$ . The Green function of the bulk Majorana is

$$G(x, t) = e^{ik_F x} \frac{v_F \pi}{2L \sin \left[ \pi(x + itv_F)/2L \right]} + e^{-ik_F x} \frac{v_F \pi}{2L \sin \left[ \pi(x - itv_F)/2L \right]}, \quad (8)$$

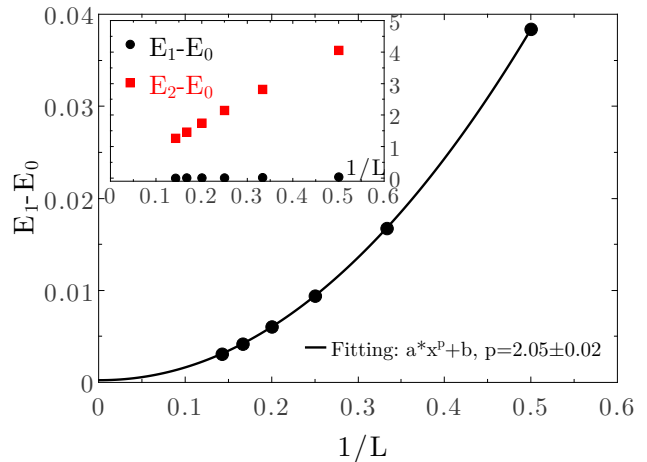


FIG. 2. Difference between the energy of the first excited and ground states,  $E_1 - E_0$ , of the three Ising chains Eqs. (3,4) as a function of the inverse of the chains length  $1/L$ . Each chain is at the critical point  $h = J$ . The strength of the coupling between chains is  $J_c = J$ . The size of the system goes from  $N = 6$  to  $N = 21$ , where  $N = 3L$ . The line fits the data to  $ax^p + b$ , where  $a$ ,  $b$  and  $p$  are free parameters. The result gives  $p = 2.05 \pm 0.05$ ,  $b = (1.0 \pm 0.5) \times 10^{-4}$  and  $a = (158.7 \pm 0.6) \times 10^{-3}$ . Inset: the black points are  $E_1 - E_0$  as a function of  $1/L$ , as in the main panel. The red squares correspond to the difference between energy of the second excited and ground states,  $E_2 - E_0$ .

where  $k_F = \pi/2$  is the Fermi wave vector and  $v_F$  is the Fermi velocity [11]. In this simpler case, the degeneracy of the spectrum is lifted by a factor  $T \sim L^{-2}$ . The effective Hamiltonian can be written as  $H_{eff} = T (f^\dagger f - 1/2)$ .

If this result holds for the full model Eq. (3,4), the existence of Majorana fermions in the JJA discussed above would be signaled by a mode with energy going as  $L^{-2}$ . The bulk eigenstates correspond to that of the Ising chain with transverse field at the critical point [18], whose energy levels scale as  $\epsilon \gtrsim 1/L$ . Then, for sufficiently long chains the unpaired Majorana are protected. We are going to check that this is actually the case for the full model Eqs. (3,4) with parameters  $J = h = J_c$ . In fact, it turns out that for the parameters chosen the low-energy doublet is still protected even in the case of short chains.

We employ numerical methods to show that our previous results are valid for the full model Eqs. (3,4). Partial diagonalizations [19] of the three Ising coupled chains are carried out for sizes ranging from  $N = 6$  to  $N = 24$ . In Fig. 2, the difference in energy between the first excited and ground-state,  $E_1 - E_0$ , appears as a function of  $1/L$ . The data have been fitted to a function  $a * x^p + b$ , where  $a, b, p$  are free parameters. The result is the solid black line with  $p = 2.05 \pm 0.05$  and  $b = (1.0 \pm 0.5) \times 10^{-4}$ . These values are in excellent agreement with our previous analysis based on RKKY interactions between Majorana particles.

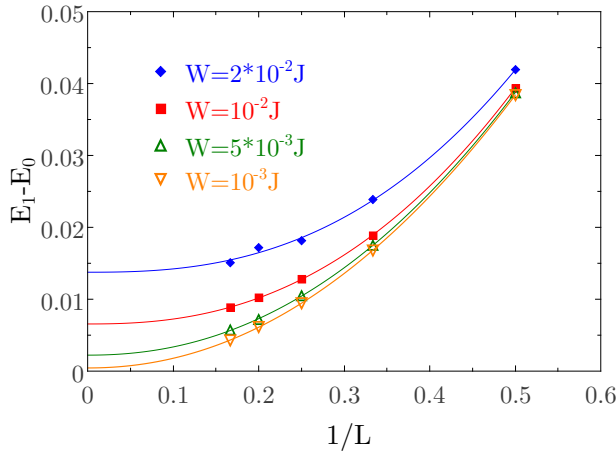


FIG. 3. Energy difference between first and ground states,  $E_1 - E_0$ , as a function of the inverse of the chains length  $1/L$ . A random magnetic field in the  $x$ -axis, following a uniform distribution in the interval  $[-W/2, W/2]$ , is added to the original Hamiltonian with  $h = J = J_c$ . Each symbol corresponds to a different  $W$ , as indicated in the legend. Lines fit each disorder to a function  $ax^p + b$ , where  $a$ ,  $b$  and  $p$  are free parameters. The value of  $b$  goes from  $b = 0.014$  to  $b = 0.0004$  and the exponent from  $p = 2.6$  to  $p = 2.07$ .

*Experimental realization.* In order to observe low energy (Majorana) doublet one can employ a set-up similar to the one used in [6]. In this set-up one registers the phase shift of a LC resonator weakly coupled to the three chains device at the frequency close to LC resonance. This phase shift depends on the state of the device. If the device is subjected to the scanning second tone, the device spectrum corresponds to the peaks in the phase shift. Furthermore, pulse excitations and shift measurements can be used to read out the state of the qubit.

Outside of the critical regime the energy of the low-energy state is large (1 – 5 GHz for the chains studied in [8]) so that it can be prepared and read out directly. Because the energy of the doublet in the protected state is very low, in order to prepare and read out the modes in this state one needs to bring the system in and out the critical regime (similar to the protected systems [20]) which can be achieved by small variation of the external field. Crucially, the lifetime of the unprotected state is expected to be long enough to allow for the readout measurements.

Low-energy doublet has to have much smaller energy than the one of higher excited states. We see in Fig. 2 that  $E_2 - E_0$  is more than two orders of magnitude larger than  $E_1 - E_0$  for  $L \sim 10$ . On the other hand the superinductors realizing the Ising chains should be sufficiently short to prevent the appearance of low energy plasmon-like modes. This does not happen for  $L < 20$ . Thus,  $L \sim 10 - 20$  is a reasonable size for experiments.

We now discuss a role of disorder present in experimental realizations. The disorder in the inter-chain couplings affects the Kondo temperature but does not change the critical behavior. We have checked this numerically by studying the model with the uniformly distributed coupling in the interval  $(J_c - 0.1J, J_c + 0.1J)$  and found that this disorder has practically no effect on the properties of the low-energy doublet.

The disorder in the chain junctions and loop fluxes is potentially more dangerous. Majorana fermion emerges as a result of renormalization process in the effective Kondo model, so it is vital to preserve the criticality of the chains assured by the condition  $J = h$ . The critical behavior is smeared if the Ising model is subject to the field,  $h_x$  in  $x$ -direction, so the presence of the random field in  $x$ -direction in the effective Ising model describing physical systems might be detrimental to the low-energy doublet. Such fields are indeed generated due to two reasons: random deviation of the loop areas and deviation of the small contacts from its average values but the latter effect disappears at  $\Phi = \Phi_0/2$ . Estimating the realistic parameters we get  $h_x \sim 10^{-3} - 10^{-2}J$ . The implementation sketched in Fig. 1 has one more potential problem: the fluxes threading the loops formed by JJ chains are large and difficult to control precisely. This flux biases the whole chain by phases  $\varphi_{1,2}$  spread over the whole chain length that change the effective value of the Josephson energies. The effect of this bias also translates into a small field  $h_x \sim 10^{-4}J$  in the Ising model.

To estimate the effect of the disorder we have studied the effect of the random fields in  $x$ -direction on the energy difference of the first two levels  $\Delta E_1$ . Fig. 3 shows the energy difference of the first two levels  $\Delta E_1(1/L)$  for the three Ising chains, Eq. (3,4), plus a small perturbation  $\Delta H_x = \sum_j \epsilon_p(j) \sigma_p^x(j)$ , where  $\epsilon_p(j)$  are randomly distributed in the interval  $[-W/2, W/2]$ . The solid lines fit each set of data to a function  $a * x^p + b$ , with free parameters  $a, b, c$ . For the largest disorder  $W = 2 * 10^{-2}J$ , the fitting function provides  $p = 2.6$  and it does not go through the origin  $b = 0.014$ . This is expected as the typical energy of the perturbation,  $W$ , is roughly the same as the one of the first level  $\Delta E$  for the largest size. The points for the smaller disorder display behavior similar to the one in the clean system. Furthermore, the low-energy mode remains in all cases well separated from the bulk spectrum in the presence of small disorder.

The numerical results can be understood qualitatively: random bulk magnetic field guarantees that the condition for criticality  $J = h$  is observed on average, thus such disorder potential in the Majorana chain does not create a spectral gap [21]. Furthermore, the Kondo effect is sensitive only to the local density of states at the impurity site, which is not strongly affected.

*Summary.* We have shown that the low-energy Majorana modes appear in a system composed by three ladders of Josephson junctions as predicted in [10]. Their



signature is a low-energy mode with energy going as  $\sim 1/L^2$ , while the bulk spectrum eigenstates have energies  $\epsilon \sim 1/L$ . We have further checked that the energy difference of the lowest doublet is more than two order of magnitude smaller than energy of bulk eigenstates for chains of length  $L \sim 10$ . So, boundary modes survive for system sizes which are accessible to experiments. Finally, we have analyzed the sources of incoherence and noise in the proposed experimental set-up. We conclude that our JJA can be a good experimental system to observe for the Majorana particle weakly (algebraically) localized at the boundary.

*Acknowledgment.* M. P. and L. B. I. acknowledge support from ARO (W911NF-13-1-0431) and ANR QuDec. A. M. T. was supported by the U.S. Department of Energy (DOE), Division of Materials Science, under Contract No. DE-AC02-98CH10886.

- 
- [1] E. Majorana, *Il Nuovo Cimento* **14**, 171 (1937).
  - [2] J. Alicea, *Reports on Progress in Physics* **75**, 076501 (2012).
  - [3] A. Y. Kitaev, *Physics-Uspekhi* **44**, 131 (2001).
  - [4] V. Mourik, K. Zuo, S. Frolov, S. Plissard, E. Bakkers, and L. Kouwenhoven, *Science* **336**, 1003 (2012).
  - [5] M. Z. Hasan and C. L. Kane, *Rev. Mod. Phys.* **82**, 3045

- (2010).
- [6] M. T. Bell, L. B. Ioffe, and M. E. Gershenson, *Phys. Rev. B* **86**, 144512 (2012).
- [7] M. T. Bell, J. Paramanandam, L. B. Ioffe, and M. E. Gershenson, *Phys. Rev. Lett.* **112**, 167001 (2014).
- [8] M. T. Bell, I. A. Sadovskyy, L. B. Ioffe, A. Y. Kitaev, and M. E. Gershenson, *Phys. Rev. Lett.* **109**, 137003 (2012).
- [9] N. Cramp and A. Trombettoni, *Nuclear Physics B* **871**, 526 (2013).
- [10] A. M. Tsvelik, *Phys. Rev. Lett.* **110**, 147202 (2013).
- [11] P. Coleman, L. B. Ioffe, and A. M. Tsvelik, *Phys. Rev. B* **52**, 6611 (1995).
- [12] A. Altland, B. Béri, R. Egger, and A. M. Tsvelik, *Phys. Rev. Lett.* **113**, 076401 (2014).
- [13] D. Giuliano and P. Sodano, *EPL (Europhysics Letters)* **103**, 57006 (2013).
- [14] M. A. Ruderman and C. Kittel, *Phys. Rev.* **96**, 99 (1954).
- [15] T. Kasuya, *Progress of Theoretical Physics* **16**, 45 (1956).
- [16] K. Yosida, *Phys. Rev.* **106**, 893 (1957).
- [17] E. Eriksson, A. Zazunov, P. Sodano, and R. Egger, *Phys. Rev. B* **91**, 064501 (2015).
- [18] P. Pfeuty, *Annals of Physics* **57**, 79 (1970).
- [19] R. B. Lehoucq, D. C. Sorensen, and C. Yang, *ARPACK users' guide: solution of large-scale eigenvalue problems with implicitly restarted Arnoldi methods*, Vol. 6 (Siam, 1998).
- [20] B. Douot and L. B. Ioffe, *Reports on Progress in Physics* **75**, 072001 (2012).
- [21] D. G. Shelton and A. M. Tsvelik, *Phys. Rev. B* **57**, 14242 (1998).